Received Date : 17-Sep-2015

Revised Date : 21-Jan-2016

Accepted Date : 25-Jan-2016

Article type : Original Research

EXAMINING THE ROLE OF SPHINGOSINE KINASE-2 IN THE REGULATION OF ENDOTHELIAL CELL BARRIER INTEGRITY

David P. Dimasi[1], Stuart M. Pitson[1,2,3], Claudine S. Bonder[1,2,3]

[1]Centre for Cancer Biology, University of South Australia and SA Pathology, Adelaide, South Australia; [2]School of Medicine, University of Adelaide, Adelaide, South Australia; [3]School of Biological Sciences, University of Adelaide, Adelaide, South Australia, AUSTRALIA

Running Title: Sphingosine kinase-2 and the vascular barrier

Funding sources: National Health and Medical Research Council (GNT1022145); Heart Foundation of Australia Fellowship to CSB and National Health and Medical Research Council Senior Research Fellowship to SMP.

Corresponding Author: Claudine Bonder

Centre for Cancer Biology, University of South Australia and SA Pathology

28 Frome Road, Adelaide, AUSTRALIA 5000

Email: claudine.bonder@unisa.edu.au

ABSTRACT

Objective: A key mediator of vascular endothelial cell barrier integrity, sphingosine-1-phosphate, is derived from phosphorylation of sphingosine by the sphingosine kinases (SK-1 and SK-2). While previous work indicates that SK-1 can regulate endothelial cell barrier integrity, whether SK-2 has a similar role remains to be determined. **Methods:** A cell impedance assay was used to assess human umbilical vein endothelial cell and bone marrow endothelial cell barrier integrity *in vitro*, with application of the SK inhibitors ABC294640, PF543, SKi and MP-A08. *In vivo* studies were conducted using intravital microscopy to assess endothelial cell barrier integrity in SK-1 (*Sphk1*$^{-/-}$) and SK-2 (*Sphk2*$^{-/-}$) knock-out mice. **Results:** Only ABC294640 and MP-A08, which can both inhibit SK-2, caused a decrease in endothelial cell barrier integrity *in vitro* in both cell types. Intravital microscopy revealed that *Sphk1*$^{-/-}$ mice had reduced endothelial cell barrier integrity compared to wild-type mice, whereas no change was evident in *Sphk2*$^{-/-}$ mice. **Conclusions:** Our data suggest that *in vitro* inhibition of SK-2 can compromise the integrity of the endothelial cell monolayer, whilst SK-1 exerts a more dominant control *in vivo.* This data may have clinical implications and could aid in the development of new treatments for disorders of vascular barrier function.

Keywords: Sphingosine-1-phosphate, sphingosine kinase, endothelial cell barrier integrity

ABBREVIATIONS

area under the curve (AUC)

dimethyl sulfoxide (DMSO)

endothelial cell (EC)

fluorescein isothiocyanate (FITC)

human umbilical vein endothelial cells (HUVEC)

sphingosine kinase-1 (SK-1)

sphingosine kinase-2 (SK-2)

sphingosine-1-phosphate (S1P)

transformed human bone marrow endothelial cells (TrHBMEC)

vascular endothelial growth factor (VEGF)

wild-type (WT)

INTRODUCTION

Vascular permeability characterises the capacity of the blood vessel wall to regulate the movement of fluid, solutes and plasma proteins out of the vasculature and into the surrounding tissue. This process is fundamentally controlled by the vascular endothelial cells (ECs), which form a continuous cellular monolayer that lines the luminal surface of blood vessels and acts as a size-selective, semi-permeable barrier between the blood plasma and the extracellular space [47]. The integrity of the vascular EC barrier is important for controlling normal physiological processes such as tissue fluid homeostasis but significant alterations in barrier integrity are associated with many inflammatory and pathological conditions, including allergic rhinitis, anaphylaxis, aberrant wound healing, cancer, edema, psoriasis and rheumatoid arthritis [19,51].

Various mediators are capable of increasing vascular permeability by generating changes in the adhesive properties of the inter-endothelial junctions. Compounds such as histamine,

bradykinin, thrombin and vascular-endothelial growth factor (VEGF) are permeability-inducing agents, acting through different signaling pathways to cause disruption of the EC barrier [32]. In contrast, mediators such as the bioactive lipid sphingosine-1-phosphate (S1P) [5], fibroblast growth factor [50] and angiopoietin-1 enhance the integrity of the EC barrier [59]. More importantly, these particular compounds play a fundamental role in regulating basal barrier integrity and are essential for protecting the EC barrier after exposure to injury or inflammatory conditions. The phospholipid S1P is a well-established pro-survival molecule and a key cell signaling mediator involved in a range of cellular processes, including cell trafficking, differentiation, angiogenesis and inflammation (as reviewed in [23,43,58,60]). S1P has a concentration in human plasma ranging from 200-400 nM [10,82] and is secreted primarily from erythrocytes and activated platelets [33] although ECs, hepatocytes, neutrophils and mast cells can also contribute to the release of S1P [79-81]. A family of five G-protein coupled receptors ($S1P_{1-5}$) bind S1P to initiate functional changes in cell signaling [24,64] . By signaling through EC expressed $S1P_1$, S1P is able to robustly maintain the integrity of the EC barrier and this is well demonstrated by numerous studies [1,5,7,11,40,46]. However, high levels of S1P can lead to signaling through $S1P_2$ or $S1P_3$, which can lead to disruption of the EC barrier [36,63].

Synthesis of S1P occurs via phosphorylation of sphingosine by the intracellular sphingosine kinases SK-1 and SK-2 [74]. Despite their common function in catalysing the biosynthesis of S1P, SK-1 and SK-2 localise to both overlapping and distinct subcellular compartments [26,30,44,57], exhibit different developmental and adult expression patterns [39,48] and are recognised to have both equivalent and alternative biological functions [26,44,73]. Whilst the role that S1P plays in maintaining EC barrier integrity is well established, the relationship between the two SK isoforms and EC barrier integrity is less defined. Previous work by our laboratory has demonstrated that siRNA knock-down of SK-1 reduced EC barrier integrity *in vitro*, which was supported by SK-1 knock-out mice (*Sphk1*$^{-/-}$) exhibiting higher

levels of vascular leakage [37]. Other studies have also reported that SK-1 activity is important for maintaining EC barrier integrity and for restoring barrier function following challenge with inflammatory agents [13,52,75]. In contrast, there is little evidence describing any link between SK-2 activity and EC barrier integrity. A study by Maines *et al* showed that administration of the SK-2 inhibitor ABC294640 was able to limit VEGF-induced increase in vascular permeability in mice [45], whilst *in vivo* studies in SK-2 knock-out (*Sphk2*$^{-/-}$) mice undergoing an anaphylactic challenge did not support this [52].

In the current study, we specifically investigated the role of SK-2 in regulating EC barrier integrity and how it may complement SK-1. A high throughput *in vitro* cell impedance based assay was employed in combination with a range of pharmacological inhibitors to SK-1 and SK-2. Data from the *in vitro* assay suggested that inhibition of SK-2 activity was more detrimental to EC barrier integrity than inhibition of SK-1. In addition to the *in vitro* studies, we used an *in vivo* model of intravital microscopy to compare EC barrier integrity in the ear microvasculature of wild-type (WT), *Sphk1*$^{-/-}$ and *Sphk2*$^{-/-}$ mice. Measurement of a fluorescent tracer revealed that *Sphk1*$^{-/-}$ mice have a compromised EC barrier, whilst the *Sphk2* $^{-/-}$ mice exhibited no difference in barrier integrity when compared to the WT mice. The novelty of these findings lies in the investigation of SK-2 functionality in the maintenance of basal EC barrier integrity, which was interrogated using both *in vivo* and *in vitro* methods. With our work also confirming a role for SK-1, these findings provide evidence to suggest that both SK isoforms could be potential therapeutic targets for conditions that exhibit aberrant vascular barrier function. Given the prevalence of conditions such as allergy, cancer and rheumatoid arthritis, wherein vascular integrity is compromised, such treatments could be of significant clinical relevance.

METHODS

Reagents

Reagents were purchased from the following suppliers: histamine, histamine-1-receptor inhibitor chlorpheniramine, histamine-2-receptor inhibitor cimetidine and fluorescein isothiocyanate (FITC) conjugated to dextran (Sigma-Aldrich, St. Louis, MO, USA); ketamine and xylazine (Lyppard, Keysborough, VIC, AUS); Lipofectamine RNAiMAX^{TM} (Life Technologies, Thermo Fisher, Carlsbad, CA, USA); SKi (also known as SKI-II, Cayman Chemical Co. Ann Arbor, MI, USA);PF543 (Tocris Bioscience, Bristol, UK). ABC294640 and MP-A08 have been described previously [17,56].

Animals

WT, *Sphk1*$^{-/-}$ and *Sphk2*$^{-/-}$ mice were on a C57Bl/6 background were generously provided by Prof. Richard Proia (NIH) and have been described previously [6,49]. Mice were housed under pathogen-free conditions at SA Pathology Animal Care Facility (South Australia, Australia). Both male and female mice were used for the intravital microscopy and were aged between 8-12 weeks of age. All experimental procedures were approved by the Animal Ethics Committee of SA Pathology and conform to the guidelines established by the 'Australian Code of Practice for the Care and Use of Animals for Scientific Purposes'.

Cell culture

The collection of human umbilical cords for use in this study was given ethical clearance from the Human Research Ethics Committee of the Children, Youth and Women's Health Service, North Adelaide, South Australia and informed written consent was obtained from all subjects in accordance with the Declaration of Helsinki. Human umbilical vein ECs (HUVEC) were isolated

as previously described [38]. Briefly, HUVEC were cultured in M199 medium (Sigma-Aldrich) containing 20% fetal bovine serum (Life Technologies), 20 mM Hepes, 2 mM glutamine, 1 mM sodium pyruvate, 1% nonessential amino acids (Cytosystems), 0.225% sodium bicarbonate, 100 U/ml penicillin and 100 µg/ml streptomycin (Gibco BRL, Paisley, Scotland). HUVEC were used at passage 2 or less for subsequent assays and were cultured in charcoal stripped fetal bovine serum, which depletes approximately 95% of the serum S1P [9]. Transformed human bone marrow ECs (TrHBMEC) were kindly supplied by Prof. Andrew Zannettino (SAHMRI, Adelaide, Australia) and have described previously [66]. The cells were cultured under the same conditions as described above for HUVEC, with the exception that the media was supplemented with heparin (Sigma-Aldrich) and endothelial growth factor (Corning, New York, USA) at 15 ng/µl.

***In vitro* EC barrier integrity assay**

To assess HUVEC and TrHBMEC barrier integrity *in vitro*, we employed the xCELLigence RTCA DP Analyzer (ACEA Biosciences, San Diego, USA), which measures fluctuations in electrical impedance when a population of cells is grown in a specialised plate (E-Plate 16)[72]. The well bottom of an E-Plate 16 (5.0 mm diameter) contains a planar gold array of electrodes which cover 80% of the surface area and permit cell attachment with or without matrices where the sensor impedance of the plate prior to cell seeding is 17 Ω ± 5 Ω at a frequency of 10 kHz. Twenty four hours after initial seeding, the wells were randomly assigned to control or treatment groups with the administration of histamine or the SK inhibitor (ABC294640, MP-A08, PF543, SKi) and the relevant vehicle (final concentration in parentheses): PF543 (≤ 0.001% DMSO), SKi and MP-A08 (≤ 0.1% DMSO); ABC294640 (≤ 0.4% methanol); Histamine (H_2O). For treatment with the histamine receptor antagonists chlorpheniramine and cimetidine, both inhibitors (at a concentration of 10 µM) were added 40 minutes prior to histamine treatment.

Changes in barrier integrity were then monitored for a further 24 hours following the addition of the inhibitor, with no change in culture media occurring during this period. Each treatment was performed in duplicate and the experiment replicated three times. For HUVEC, all replicates were performed on biologically different donor cultures with the gender of these cells unknown as the donors were de-identified.

Intravital microscopy

Intravital microscopy to measure *in vivo* barrier integrity of the mouse ear vasculature was performed as described previously [14]. Mice were sedated using an intra-peritoneal injection of a 10 mg/ml ketamine/xylazine mixture at a dosage of 1 µl per gram. The mouse ear was then placed over a raised platform and mounted under a glass coverslip in preparation for imaging. Prior to imaging, the mouse was allowed to rest for 30 minutes to reduce any potential inflammation that may have resulted from the manual handling. To visualise the vasculature, 100 µl of 10 mg/ml FITC-dextran (150, 70 or 40 kDa) was injected intravenously via an intra-orbital injection. The mouse ear was then positioned under a 20x objective within a heated chamber of an LSM 710 two-photon microscope (Carl Zeiss, Jena, Germany). The FITC-Dextran was excited using a tuneable Mai Tai Ti:Sapphire multiphoton laser (Spectra-Physics, Santa Clara, USA) and external non-descanned detectors were used to capture the fluorescence signal. A stack of 3 images over a range of 10 µm was then acquired every 5 minutes over the course of 15 minutes. Image analysis was undertaken using a macro written for use within Image J [61]. As all images were in color, the green channel was split out and then a median filter with a radius of 2.0 pixels was employed to reduce noise. A fluorescence threshold was then manually applied by the user to the time zero image, with subsequent images in the series then using the threshold values from the time zero image. Image analysis then determined the percentage area covered by the threshold region. For analysis of average vessel diameter, measurements were taken from the

time zero image of each mouse using Image J. Vessels were defined as small (less than 8 μm diameter), medium (8-13 μm diameter) or large (> 13 μm diameter). The number of vessels within each group was then counted and calculated as a proportion of the total number of vessels in that image.

Statistical analysis

Immediately prior to each independent EC barrier integrity assay experiment being conducted we confirmed that the 'cell index' values between wells was statistically similar. In addition, at the time of reagent administration, cell index values were normalised to a value of '1' to overcome the 0.005±0.005 variances in cell index readings that was observed between wells to better provide direct comparison across treatment groups. An area under the curve (AUC) analysis was undertaken to compare the cell index values of the treatments and the vehicle. AUC values were then compared using a two-tailed Student's t-test, with $p < 0.05$ being accepted as statistically significant.

For the intravital analysis, the percentage fluorescent area from each image within a series was normalised back to the time zero image, with the normalised fluorescent area then plotted against time. A two-way repeated measures ANOVA was performed to compare the rate of leakage of the fluorescent dye in the WT, *Sphk1*$^{-/-}$ and *Sphk2*$^{-/-}$ mice. To compare the proportion of vessels within each size range across different mouse genotypes, a Kruskal-Wallis test was utilised. Statistical significance was accepted as $p < 0.05$.

RESULTS

Histamine rapidly induces a decrease in HUVEC barrier integrity

The role of histamine in inducing EC permeability is well-established and as a consequence it was used in this study to establish the validity of measuring EC barrier integrity *in vitro* using the xCELLigence RTCA DP Analyzer. In the first instance, HUVEC were seeded into the gelatin-coated E-Plate 16 at concentrations of 0.5, 1.0, 2.5 and $5x10^4$ cells per well to determine optimal seeding densities. As shown in Figure 1A, within 6 hours of seeding, the $\geq 1 \times 10^4$ cell containing wells formed a stable, and likely confluent, monolayer as indicated by a plateau of the impedance profile; quantitatively calculated and expressed by the xCELLigence software as the 'cell index' (a dimensionless parameter derived as a relative change in measured electrical impedance to represent cell status[72]). Also established in these experiments, was that the impedance readings of 'cell free' wells remained significantly lower (Figure 1A). In subsequent experiments (wherein $2.5x10^4$ cells seeded each well) we confirmed that no differences in basal cell layer resistance existed across the wells prior to proceeding with each cell containing well maintaining a comparable and constant cell index for the two hours prior to testing. In fact, we repeatedly observed that the cell containing wells varied by approximately 0.005±0.005 cell index units at time of treatment. Following establishment of the HUVEC monolayer, we used published methods [73] to reveal that cells treated with 12.5 μM histamine undergo a rapid and significant decrease in barrier integrity when compared to the vehicle control (Figure 1B). This loss in barrier integrity equated to a peak fall in cell index of 47 ± 1.4% after only 2.5 minutes. After approximately 20 minutes, the cell index of the histamine-treated cells had recovered to the baseline level exhibited by the vehicle treated cells (Figure 1B), highlighting the transient nature of this effect and demonstrating that the treatment was not cytotoxic. To confirm specificity, HUVEC were pre-treated with the known histamine-1-receptor inhibitor chlorpheniramine (10

μM) [70] 40 minutes prior to treatment with 12.5 μM histamine (Figure 1C). Pre-treatment with chlorpheniramine was able to completely abolish the fall in barrier integrity seen with histamine treatment alone. In addition, HUVEC were also pre-treated with the known histamine-2-receptor inhibitor cimetidine (10 μM) [70], this had no effect on reducing histamine-induced loss of barrier integrity (Figure 1D). Quantified data from independent experiments using three different biological HUVEC donors showed via area under the curve (AUC) calculations that pre-treatment with the H1R inhibitor (chlorpheniramine) significantly inhibited histamine-induced loss of barrier integrity (Figure 1E).

The SK-1 inhibitor PF543 has a modest effect on HUVEC barrier integrity

To investigate whether inhibition of SK-1 could disrupt basal EC barrier integrity *in* vitro, the commercially available SK-1-selective inhibitor PF543 was administered to HUVEC monolayers. PF543 was administered at concentrations of 10 nM, 25 nM, 50 nM and 100 nM (Figure 2A-E), which was based on a K_i of 3.6 nM [65]. At all concentrations, PF543 was able to induce a modest but significant decrease in HUVEC barrier integrity. A concentration-related response was evident, with the largest decrease in barrier integrity occurring with the 100 nM treatment with a 20 ± 5% fall in the cell index after approximately 25 minutes. To note, at all concentrations of PF543, the cell index of the treated cells returned to baseline levels over the course of a few hours, suggesting that the effect was transient and not cytotoxic (Supplementary Figure 1).

The SK-2 inhibitor ABC294640 decreased HUVEC barrier integrity

Next we utilised a commercially available SK-2-selective inhibitor, ABC294640, in the *in vitro* HUVEC barrier integrity assay. Given that the K_i for ABC294640 is 9.8 μM [17], we administered the inhibitor at concentrations ranging from 5 μM to 40 μM. Whilst no effect was

evident at 5 μM and 10 μM, the higher concentrations of 20 μM and 40 μM were able to induce a significant decrease in HUVEC barrier integrity (Figure 3). Notably, treatment with 40 μM of ABC294640 resulted in a 73 ± 16% decrease in cell index readings within 15 minutes, which was the largest reduction seen with any of the inhibitors used in this study. However, it is possible that at a concentration of 40 μM, ABC294640 is slightly cytotoxic, as cell index readings do not return to baseline levels after 12 hours in culture (Supplementary Figure 2). This effect may be attributed to the 0.4% methanol vehicle used for this compound as cytotoxicity was not evident at the lower concentrations of ABC294640 (Supplementary Figure 2).

Combination of PF543 and ABC294640 enhances the decrease in HUVEC barrier integrity

In order to further establish whether simultaneous inhibition of both SK-1 and SK-2 can have a more potent impact on EC barrier integrity, a combination treatment of PF543 and ABC294640 was employed. Both inhibitors were used at their optimal concentration as derived from the previous experiments, with PF543 at 100 nM and ABC294640 at 20 μM. The ABC294640 concentration was chosen as it did not exhibit any cytotoxic effects as opposed to 40 μM. As shown in Figure 4, treatments with PF543 and ABC294640 alone were 20 ± 9% and 12 ± 7%, respectively. In contrast, the combined treatment with PF543 and ABC294640 resulted in a 32 ± 6% decrease in cell index, demonstrating an additive effect. There was no evidence that any of these treatments exhibited any long-term cytotoxicity (Supplementary Figure 3).

SK-1/2 inhibitors have varying effects on HUVEC barrier integrity

Whilst initially considered to be an exclusive inhibitor of SK-1, SKi has recently been demonstrated to inhibit both SK-1 and SK-2, with a K_i of 16 μM and 7.9 μM respectively [18]. In contrast to both PF543 and ABC294640, SKi was unable to elicit a significant change in HUVEC barrier integrity at concentrations ranging from 5 μM to 40 μM (Figure 5). There was

no evidence of long-term cell toxicity following administration of SKi (Supplementary Figure 4). In addition to SKi, another SK-1/2 inhibitor, MP-A08, was also investigated in the *in vitro* HUVEC barrier integrity assay. MP-A08 exhibits a higher affinity for SK-2 than SK-1, with K_i values of 6.9 μM and 27 μM respectively [56]. We administered MP-A08 at concentrations ranging from 5 μM to 40 μM, with the higher concentrations of 20 μM and 40 μM inducing a significant decrease in HUVEC barrier integrity (Figure 6). Treatment with 40 μM of MP-A08 resulted in a 30 ± 7% decrease in cell index readings after approximately 15 minutes, which was the second most potent response from any of the inhibitors used in this study. As with both PF543 and ABC294640, the cell index readings of the HUVEC treated with MP-A08 returned to baseline levels over the course of a few hours, suggesting that the effect of the inhibitor is transient and that there are no cytotoxic effects (Supplementary Figure 5). To note, at a concentration of 40 μM, both the SKi and MP-A08 treatments contain a final DMSO concentration of ~0.1%, which could have transient effects of EC barrier integrity as seen in the vehicle only treatments (Figure 5D and 6D).

The SK inhibitors have varying effects on TrHBMEC barrier integrity

As variation is known to exist between ECs which are isolated from different vascular beds [3,4], we tested the response of the human bone marrow derived microvascular TrHBMEC cell line to the SK inhibitors. All inhibitors were examined at the optimal concentration as determined from the aforementioned HUVEC data: PF543 at 100 nM; ABC294640 at 20 μM; SKi at 40 μM; MP-A08 at 40 μM. Figure 7 shows that there was no evidence for changes in barrier integrity in response to treatment with either PF543 or SKi. In contrast, with ABC294640, a significant decrease in barrier integrity was observed, with a peak fall in cell index of 20 ± 5% (Figure 7). An even more pronounced effect on barrier integrity was observed with MP-A08, which caused a 39 ± 4% fall in cell index. Prolonged incubation of the TrHBMEC with the inhibitors suggested

that only SKi had cytotoxic effects on the cells after approximately 6 hours in culture (Supplementary Figure 6).

Sphk1$^{-/-}$ but not _Sphk2_$^{-/-}$ mice have compromised microvascular barrier integrity

Intravital microscopy was used to compare the barrier integrity of the ear microvasculature of _Sphk1_$^{-/-}$, _Sphk2_$^{-/-}$ mice and their WT counterparts *in vivo*. To note, our previous findings demonstrated that _Sphk1_$^{-/-}$ mice have reduced microvascular barrier integrity in the back skin when using the Miles assay, which utilises Evans blue dye [37] but here we employed the much more sensitive approach of intravital microscopy. This technique allowed us to examine changes in permeability over time within live (anesthetised) mice using three different sizes of a FITC-Dextran tracer [14]. The largest molecule administered was a 150 kDa FITC-Dextran, which under basal conditions is reportedly too large to pass through the EC barrier [14]. Similarly, the 70 kDa FITC-Dextran is too large to pass through the vasculature under basal conditions, although some slight movement of the molecule into the interstitial space can be expected [14]. The 40 kDa FITC-Dextran is small enough to move through the EC barrier under basal conditions and it is predicted to undergo a mild but sustained leakage over the course of the 15 minute imaging window [14].

As shown in Figure 8, with administration of the 150 kDa FITC-Dextran, the tracer is confined within the vasculature in the WT, _Sphk1_$^{-/-}$ and _Sphk2_$^{-/-}$ mice and undergoes little or no leakage into the interstitial space over the course of 15 minutes. There was no significant difference in the rate of leakage between these mice, which was assessed by determining the normalised total fluorescence area of each image at every time point (Figure 8D). Similarly, minimal leakage was observed following injection of the 70 kDa FITC Dextran in the WT and Sphk2$^{-/-}$ mice (Figure 9). In stark contrast, substantial leakage of the 70 kDa FITC Dextran into the interstitial space was observed in the _Sphk1_$^{-/-}$ group over the course of the 15 minutes (Figure

9). Shown in Figure 9E, the differences in leakage of the 70 kDa FITC-Dextran tracers in the WT and *Sphk1*$^{-/-}$ mice was not based on gender variation. A similar result was observed with the 40 kDa FITC-Dextran tracer, with the *Sphk1*$^{-/-}$ mice exhibiting a significantly increased rate of leakage (Figure 10). As anticipated, the 40 kDa FITC-Dextran tracer was still able to move into the interstitial space in the WT and *Sphk2*$^{-/-}$ mice, although at a reduced rate compared to that observed in the *Sphk1*$^{-/-}$ mice (Figure 10). To note, we observed no differences in the proportion of small, medium or large diameter vessels across the different mouse strains for all sizes of FITC-Dextran examined (Supplementary Figure 7). The only exception was within the small proportion of large vessels in the 70 kDa FITC-Dextran group, where a slight reduction in *Sphk2*$^{-/-}$ numbers was detected (Supplementary Figure 7B). However, this may be an artefact generated by the small sample size in this experiment.

DISCUSSION

The regulated passage of blood stream components into the interstitial space is a fundamental physiological function that is facilitated by the ECs that line the vasculature. Under both basal and inducible conditions, vascular EC barrier integrity is tightly controlled and can be regulated by a range of mediators. Despite increasing knowledge of the pathways involved in controlling EC barrier integrity, much remains unknown about this essential feature of the vascular system. This study aimed to investigate what role the two SK isoforms play in the maintenance of basal vascular EC barrier integrity, which was interrogated through the novel *in vitro* use of inhibitors to SK-1 and SK-2 and by applying state-of-the art intravital microscopy *in vivo*. For the first time, we were able to demonstrate, through the use of pharmacological inhibitors, that SK-2 activity is important for sustaining HUVEC and TrHBMEC barrier integrity *in vitro*. However, experiments conducted on *Sphk2*$^{-/-}$ mice using intravital microscopy demonstrated that ablation of

this gene had no effect on EC barrier integrity while our data supported previous documentation of *Sphk1*$^{-/-}$ mice having a compromised EC barrier [13,37,52,75].

The *in vitro* measurement of EC barrier integrity in this study was undertaken using an xCELLigence RTCA DP Analyzer, which employs electrical impedance-based technology to assess a range of cellular parameters. This technique was first described by Giaever and Keese [20,21], with the technology subsequently adapted for the xCELLigence platform [72]. The use of this methodology to assess changes in EC barrier integrity has been well-described and offers several advantages over the alternative transwell assay, including the ability to monitor changes in barrier integrity in real-time and without the use of a label [12,31,34,35,69,76]. In order to establish whether this assay would be applicable to assessing the barrier integrity of our EC cultures, HUVEC were treated with the inflammatory mediator histamine, which is known to induce disruption of the EC barrier [41]. Our data indicated that histamine caused a rapid but transient decrease in HUVEC barrier integrity and that this effect was mediated by signaling through the histamine-1-receptor, which has been reported previously [62]. These findings validated the use of our HUVEC donor cultures and the xCELLigence RTCA DP Analyzer to assess EC barrier integrity *in vitro*.

To assess if SK-1 and SK-2 activity is important for the maintenance of EC barrier integrity *in vitro*, experiments using pharmacological inhibitors were undertaken. To inhibit SK-1 alone, PF543 was utilised, which is a sphingosine-competitive inhibitor that is 100-fold more selective for SK-1 than SK-2 and is described as the most potent inhibitor of SK-1 currently available [65]. We observed that PF543 caused a relatively small but significant decrease in barrier integrity at concentrations ranging from 10 nM to 100 nM. To-date, this is the only description of PF543 being used in this capacity. Inhibition of SK-2 was undertaken using the compound ABC294640, which acts as a competitive inhibitor with respect to sphingosine and exhibits strong selectivity towards SK-2 [17]. Our data indicated that treatment with ABC294640

caused a significant, but transient, reduction in HUVEC barrier integrity that was quantitatively larger than that seen with the SK-1 inhibitor PF-543. When both these inhibitors were combined, there was compelling evidence of an additive effect, further illustrating how both SK isoforms play an important role in the maintenance of EC barrier integrity.

In addition to PF543 and ABC294640, which preferentially inhibit specific SK isoforms, we utilised two compounds that have activity against both SK-1 and SK-2. SKi (also referred to as SKI-II), is a sphingosine-competitive inhibitor of both SK-1 and SK2 [15,18]. There was no evidence from our data that SKi (5-40 μM) had any effect on EC barrier integrity, which is supported by Itagaki *et al*, who observed that SKi did not alter basal HUVEC barrier integrity *in vitro* using a transwell assay [27]. Along with SKi, we also utilised MP-A08, a recently developed inhibitor of both SK-1 and SK-2 [56]. As with ABC294640, the significant reduction in EC barrier integrity seen with MP-A08 treatment at 40 μM was larger than that observed with PF543. Given that MP-A08 preferentially targets SK-2 [56], this supports our findings that pharmacological inhibition of SK-2 causes a disruption of EC barrier integrity *in vitro*. Importantly, our previous data demonstrating that HUVEC possess comparable levels of SK-1 and SK-2 activity [73], suggest that the observed preferential role for SK-2 is not simply a result of predominance of this isoform in these cells.

Given the significant phenotypic heterogeneity that exists between different EC types isolated from different vascular beds [3,4], we also evaluated the response of the microvascular TrHBMEC line to the SK inhibitors. Characterization of the TrHBMEC demonstrates that they exhibit the classical hallmarks of ECs, including expression of von Willebrand factor, P-selectin and CD31 and up-take of acetylated low-density lipoprotein [66]. Both ABC294640 and MP-A08 induced a significant reduction in barrier integrity that was reminiscent of the data obtained from the HUVEC. Furthermore, SKi did not have any impact on barrier integrity, which was also in accordance with what was observed in HUVEC. In contrast to the HUVEC results however,

PF543 was not able to elicit a reduction in TrHBMEC barrier integrity. As the inhibitors behaved in a largely similar manner in disrupting the barrier integrity of large vessel ECs (represented by our primary HUVEC) and microvascular ECs (represented by the TrHBMEC cell line), the data from ABC294640 and MP-A08 suggest that SK-2 may play a more prominent role than SK-1 in the maintenance of EC barrier integrity across a range of vascular beds. This advances our current knowledge as we reveal an immediate response of the basal EC barrier integrity to SK inhibitors. This differs from other documented manipulation of SK *in vitro* wherein ECs (derived from large and/or small vessels) were treated with SK inhibitors (e.g. DMS and SKi) prior to stimulation with pro-inflammatory mediators, prevented (i) the disruption of barrier integrity by thrombin [28] and (ii) the increased barrier integrity by angiopoietin-1 [37]. Whether the SK inhibitors had an effect independent of thrombin or angiopoietin-1 in these experiments was not shown. Taken together, there is increasing evidence for an important and complex role for SK in the integrity of the vasculature that is yet to be clearly defined.

In recent years, there has been widespread interest in the use of SK inhibitors as therapeutics for a variety of conditions, most notably cancer (reviewed in [55]). Many inhibitors are currently being evaluated in pre-clinical or clinical trials, with the structural sphingosine analogue FTY720 (also known as fingolimod and Gilenya^{TM}) approved for use as a treatment for multiple sclerosis [70]. Of the inhibitors used in this study, ABC294640 is currently undergoing a phase I/IIa clinical trial for the treatment of patients with diffuse large B cell lymphoma and has also shown potential as a therapeutic for prostate cancer [78], whilst SKi and MP-A08 have documented anti-cancer properties [16,56]. Interestingly, a relatively new class of anti-cancer drugs termed vascular-disrupting agents act by inducing increased vascular permeability within a tumor, thus restricting blood flow and the delivery of nutrients [77]. Given the permeability-inducing properties of the SK inhibitors investigated here, it is possible that this mode-of-action might improve the efficacy of these agents as anti-tumor compounds. However, as tumor

vasculature is notoriously tortuous and leaky whether these agents further influence EC barrier integrity in this context remains to be determined. In addition, any possible side-effects that could result from increased vascular permeability must also be considered, including the potential for complications associated with edema [2].

Previous studies have demonstrated that SK-1 activity is important for EC barrier integrity *in vivo*, with *Sphk1*$^{-/-}$ mice exhibiting a higher propensity for microvascular leakage under both basal and inflammatory states [13,37,52,75]. However, in contrast to the work undertaken here, none of these studies employed fluorescence-based intravital microscopy to assess microvascular integrity. The use of two-photon intravital microscopy to assess microvascular leakage offers real-time, high resolution imaging of fluorescent molecules in living tissues with little or no tissue damage [83]. This affords significant advantages over other techniques to assess microvascular permeability *in vivo*, such as the Miles assay, which is not suited to assessing permeability of various protein sizes over time under basal conditions within the same mice [14]. By employing *Sphk1*$^{-/-}$ mice, we were able to verify the use of this methodology within our laboratory by offering a comparison to known data. To examine whether SK-2 also contributes to EC barrier integrity *in vivo*, we utilised a *Sphk2*$^{-/-}$ strain that does not show any overt phenotype, with these mice being fertile and viable to at least 12 months of age [6,49]. Our study demonstrates that for the 150 kDa, 70 kDa and 40 kDa FITC-Dextran tracers however, there was no difference in the rate of basal leakage between the WT and *Sphk2*$^{-/-}$ mice. In contrast, we did observe a significant loss of EC barrier integrity in the *Sphk1*$^{-/-}$ mice when both the 70 kDa and 40 kDa FITC-Dextran were administered. Our results support previous findings of reduced blood vessel integrity in the *Sphk1*$^{-/-}$ mice [13,37,52,75] and demonstrate for the first time that *Sphk2*$^{-/-}$ mice have normal microvascular barrier integrity. This data verifies the earlier work of Olivera *et al*, who failed to find any evidence of increased microvascular permeability in the lungs of *Sphk2*$^{-/-}$ mice undergoing an anaphylaxis challenge [52]. It is

important to note that *Sphk1*$^{-/-}$ mice have approximately half the level of plasma S1P when compared to WT mice [6,29,53], whilst *Sphk2*$^{-/-}$ mice have a significantly higher level of plasma S1P than their WT counterparts [29,53,67]. Evidence from Sensken *et al* suggests that impaired transport of S1P out of the bloodstream and into the lymph circulation in *Sphk2*$^{-/-}$ mice is responsible for the elevated plasma S1P [67], although increases in SK-1 activity or decreases in S1P lyase or lipid phosphate phosphatase activity could also play a role. Given that S1P is a key mediator of EC barrier integrity [5,7,11,40,46], it is likely that the reduced levels of S1P in the *Sphk1*$^{-/-}$ mice are responsible for the increased leakage of the FITC-Dextran tracer seen in these animals. The elevated plasma S1P found in *Sphk2*$^{-/-}$ mice would also explain the normal EC barrier integrity we found in this study. Despite increases in S1P having been shown to mediate higher VEGF expression in ECs *in vitro* [25], the subsequent increase in microvascular permeability that would result from VEGF secretion was not observed here.

It is evident from our data that a discrepancy exists between the SK-2 results from the *in vitro* and *in vivo* experiments. It is conceivable that the *in vitro* inhibitor data represents an intracellular mechanism of SK-1 and SK-2 action or the S1P they generate, as the effects of inhibitor addition are immediate (i.e. within seconds). With respect to SK-2, treatment of HUVEC with ABC294640 and MP-A08 could potentially reduce the level of secreted S1P, which would in turn decrease signaling through $S1P_1$. However, it is possible that this mechanism does not account for all the changes in EC barrier integrity observed within our study. Intracellular targets of S1P have been identified and include histone deacetylases [22], tumor necrosis factor receptor-associated factor 2 [8], prohibitin-2 [71], peroxisome proliferator activated receptor-γ [54] and possibly p-21 activated kinase 1 [42]. If S1P directly interacts with an intracellular pathway that regulates adhesion molecule interactions, then disruption of this pathway via inhibition of SK-2 could potentially weaken cell-cell contacts. In addition, given that SK-2 localises to organelles independently of SK-1, such as the nucleus, mitochondria and

endoplasmic reticulum, S1P produced at these sites is likely to act on targets in close proximity and not be secreted from the cell [68]. In contrast to this proposed intracellular mode of action, findings from the *Sphk2*$^{-/-}$ mouse are likely the result of elevated levels of S1P-induced $S1P_1$ mediated signaling [5,7,11,39], the effects of which may override any deficit in intracellular SK-2. It is also conceivable that some of the disparity seen between the *in vitro* and *in vivo* data could represent species differences in the regulation of EC barrier integrity by the sphingolipid pathway, although this would require further investigation.

In summary, our findings reveal a role for SK-2, via pharmacological manipulation, in the regulation of EC barrier integrity. Through use of the inhibitors ABC294640 and MP-A08, we were able to present for the first time *in vitro* data showing a potential link between SK-2 activity and HUVEC and TrHBMEC barrier integrity. In addition, our study was able to confirm a role for SK-1 in the regulation of EC barrier integrity, through the novel *in vitro* use of inhibitors PF543 and MP-A08 and by employing intravital microscopy on *Sphk1*$^{-/-}$ mice. An improved understanding of the molecular pathways that regulate the EC barrier is of great importance, as dysfunctional control of this facet of the vascular system can contribute to the onset or progression of many pathological states. Increases in vascular permeability are associated with many clinically relevant conditions including allergy, anaphylaxis, cancer, edema and several auto-immune diseases. There is an urgent requirement for improved treatments for many of these disorders and inducing changes in vascular permeability may offer an attractive therapeutic strategy. To this end, pharmacologically targeting SK-1 and/or SK-2 to alter their activity may prove to be a viable approach to generating clinically beneficial changes in the EC barrier.

ACKNOWLEDGEMENTS

The authors wish to thank Dr. Michael Michael and Hayley McFetridge for their assistance with the use of the xCELLigence RTCA DP Analyser, Brenton Ebert for his design of the Image J macro and Prof Michael Hickey for assistance with the intravital microscopy.

PERSPECTIVES

David Dimasi: Our knowledge of the mechanisms that control vascular EC barrier integrity is incomplete. The study provides evidence that SK-2 may be a novel regulator of EC barrier integrity, although further work is required. This finding could have important clinical applications, particularly in the treatment of conditions such as allergy, anaphylaxis, cancer and edema.

Stuart Pitson: SK-2 is an enigmatic enzyme, with many of its true roles in mammalian biology yet to be clearly determined. In this study we provide *in vitro* evidence for a potential role for SK-2 in the control of vascular integrity. This, however, was not recapitulated in knockout mouse studies, highlighting the complex nature of this enzyme and its interplay with SK-1 and control of circulating S1P.

Claudine Bonder: Increasing vascular permeability is a fundamental feature of inflammation and contributes to tumor metastasis. The SK/S1P/receptor axis is central to controlling EC barrier integrity and whilst immediate responses to pharmacological compounds by EC monolayers *in vitro* support a unified role for SK-1 and SK-2, the redundancy observed *in vivo* supports the complex nature of this system which is not singularly overcome.

REFERENCES

1. Adamson RH, Sarai RK, Altangerel A, Thirkill TL, Clark JF, Curry FR. Sphingosine-1-phosphate modulation of basal permeability and acute inflammatory responses in rat venular microvessels. *Cardiovascular research* **88**: 344-351, 2010.

2. Agostoni A, Cicardi M, Porreca W. Peripheral edema due to increased vascular permeability: a clinical appraisal. *Int J Clin Lab Res* **21**: 241-246, 1992.

3. Aird WC. Phenotypic heterogeneity of the endothelium: I. Structure, function, and mechanisms. *Circulation research* **100**: 158-173, 2007.

4. Aird WC. Phenotypic heterogeneity of the endothelium: II. Representative vascular beds. *Circulation research* **100**: 174-190, 2007.

5. Allende ML, Proia RL. Sphingosine-1-phosphate receptors and the development of the vascular system. *Biochimica et biophysica acta* **1582**: 222-227, 2002.

6. Allende ML, Sasaki T, Kawai H, Olivera A, Mi Y, van Echten-Deckert G, Hajdu R, Rosenbach M, Keohane CA, Mandala S, Spiegel S, Proia RL. Mice deficient in sphingosine kinase 1 are rendered lymphopenic by FTY720. *The Journal of biological chemistry* **279**: 52487-52492, 2004.

7. Allende ML, Yamashita T, Proia RL. G-protein-coupled receptor S1P1 acts within endothelial cells to regulate vascular maturation. *Blood* **102**: 3665-3667, 2003.

8. Alvarez SE, Harikumar KB, Hait NC, Allegood J, Strub GM, Kim EY, Maceyka M, Jiang H, Luo C, Kordula T, Milstien S, Spiegel S. Sphingosine-1-phosphate is a missing cofactor for the E3 ubiquitin ligase TRAF2. *Nature* **465**: 1084-1088, 2010.

9. Bonder CS, Sun WY, Matthews T, Cassano C, Li X, Ramshaw HS, Pitson SM, Lopez AF, Coates PT, Proia RL, Vadas MA, Gamble JR. Sphingosine kinase regulates the rate of endothelial progenitor cell differentiation. *Blood* **113**: 2108-2117, 2009.

10. Caligan TB, Peters K, Ou J, Wang E, Saba J, Merrill AH, Jr. A high-performance liquid chromatographic method to measure sphingosine 1-phosphate and related compounds from sphingosine kinase assays and other biological samples. *Analytical biochemistry* **281**: 36-44, 2000.

11. Camerer E, Regard JB, Cornelissen I, Srinivasan Y, Duong DN, Palmer D, Pham TH, Wong JS, Pappu R, Coughlin SR. Sphingosine-1-phosphate in the plasma compartment regulates basal and inflammation-induced vascular leak in mice. *The Journal of clinical investigation* **119**: 1871-1879, 2009.

12. Chen XL, Nam JO, Jean C, Lawson C, Walsh CT, Goka E, Lim ST, Tomar A, Tancioni I, Uryu S, Guan JL, Acevedo LM, Weis SM, Cheresh DA, Schlaepfer DD. VEGF-induced vascular permeability is mediated by FAK. *Developmental cell* **22**: 146-157, 2012.

13. Di A, Kawamura T, Gao XP, Tang H, Berdyshev E, Vogel SM, Zhao YY, Sharma T, Bachmaier K, Xu J, Malik AB. A novel function of sphingosine kinase 1 suppression of JNK activity in preventing inflammation and injury. *The Journal of biological chemistry* **285**: 15848-15857, 2010.

14. Egawa G, Nakamizo S, Natsuaki Y, Doi H, Miyachi Y, Kabashima K. Intravital analysis of vascular permeability in mice using two-photon microscopy. *Scientific reports* **3**: 1932, 2013.

15. French KJ, Schrecengost RS, Lee BD, Zhuang Y, Smith SN, Eberly JL, Yun JK, Smith CD. Discovery and evaluation of inhibitors of human sphingosine kinase. *Cancer research* **63**: 5962-5969, 2003.

16. French KJ, Upson JJ, Keller SN, Zhuang Y, Yun JK, Smith CD. Antitumor activity of sphingosine kinase inhibitors. *The Journal of pharmacology and experimental therapeutics* **318**: 596-603, 2006.

17. French KJ, Zhuang Y, Maines LW, Gao P, Wang W, Beljanski V, Upson JJ, Green CL, Keller SN, Smith CD. Pharmacology and antitumor activity of ABC294640, a selective inhibitor of sphingosine kinase-2. *The Journal of pharmacology and experimental therapeutics* **333**: 129-139, 2010.

18. Gao P, Peterson YK, Smith RA, Smith CD. Characterization of isoenzyme-selective inhibitors of human sphingosine kinases. *PloS one* **7**: e44543, 2012.

19. Garcia JG. Concepts in microvascular endothelial barrier regulation in health and disease. *Microvascular research* **77**: 1-3, 2009.

20. Giaever I, Keese CR. Monitoring fibroblast behavior in tissue culture with an applied electric field. *Proceedings of the National Academy of Sciences of the United States of America* **81**: 3761-3764, 1984.

21. Giaever I, Keese CR. Micromotion of mammalian cells measured electrically. *Proceedings of the National Academy of Sciences of the United States of America* **88**: 7896-7900, 1991.

22. Hait NC, Allegood J, Maceyka M, Strub GM, Harikumar KB, Singh SK, Luo C, Marmorstein R, Kordula T, Milstien S, Spiegel S. Regulation of histone acetylation in the nucleus by sphingosine-1-phosphate. *Science* **325**: 1254-1257, 2009.

23. Hannun YA, Obeid LM. Principles of bioactive lipid signalling: lessons from sphingolipids. *Nature reviews Molecular cell biology* **9**: 139-150, 2008.

24. Hanson MA, Roth CB, Jo E, Griffith MT, Scott FL, Reinhart G, Desale H, Clemons B, Cahalan SM, Schuerer SC, Sanna MG, Han GW, Kuhn P, Rosen H, Stevens RC. Crystal structure of a lipid G protein-coupled receptor. *Science* **335**: 851-855, 2012.

25. Heo K, Park KA, Kim YH, Kim SH, Oh YS, Kim IH, Ryu SH, Suh PG. Sphingosine 1-phosphate induces vascular endothelial growth factor expression in endothelial cells. *BMB Rep* **42**: 685-690, 2009.

26. Igarashi N, Okada T, Hayashi S, Fujita T, Jahangeer S, Nakamura S. Sphingosine kinase 2 is a nuclear protein and inhibits DNA synthesis. *The Journal of biological chemistry* **278**: 46832-46839, 2003.

27. Itagaki K, Yun JK, Hengst JA, Yatani A, Hauser CJ, Spolarics Z, Deitch EA. Sphingosine 1-phosphate has dual functions in the regulation of endothelial cell permeability and Ca2+ metabolism. *The Journal of pharmacology and experimental therapeutics* **323**: 186-191, 2007.

28. Itagaki K, Zhang Q, Hauser CJ. Sphingosine kinase inhibition alleviates endothelial permeability induced by thrombin and activated neutrophils. *Shock* **33**: 381-386, 2010.

29. Kharel Y, Raje M, Gao M, Gellett AM, Tomsig JL, Lynch KR, Santos WL. Sphingosine kinase type 2 inhibition elevates circulating sphingosine 1-phosphate. *The Biochemical journal* **447**: 149-157, 2012.

30. Kleuser B, Maceyka M, Milstien S, Spiegel S. Stimulation of nuclear sphingosine kinase activity by platelet-derived growth factor. *FEBS letters* **503**: 85-90, 2001.

31. Kobayashi K, Tsubosaka Y, Hori M, Narumiya S, Ozaki H, Murata T. Prostaglandin D2-DP signaling promotes endothelial barrier function via the cAMP/PKA/Tiam1/Rac1 pathway. *Arteriosclerosis, thrombosis, and vascular biology* **33**: 565-571, 2013.

32. Komarova Y, Malik AB. Regulation of endothelial permeability via paracellular and transcellular transport pathways. *Annual review of physiology* **72**: 463-493, 2010.

33. Ksiazek M, Chacinska M, Chabowski A, Baranowski M. Sources, metabolism, and regulation of circulating sphingosine-1-phosphate. *Journal of lipid research* **56**: 1271-1281, 2015.

34. Kustermann S, Manigold T, Ploix C, Skubatz M, Heckel T, Hinton H, Weiser T, Singer T, Suter L, Roth A. A real-time impedance-based screening assay for drug-induced vascular leakage. *Toxicological sciences : an official journal of the Society of Toxicology* **138**: 333-343, 2014.

35. Li HB, Ge YK, Zhang L, Zheng XX. Astragaloside IV improved barrier dysfunction induced by acute high glucose in human umbilical vein endothelial cells. *Life sciences* **79**: 1186-1193, 2006.

36. Li Q, Chen B, Zeng C, Fan A, Yuan Y, Guo X, Huang X, Huang Q. Differential activation of receptors and signal pathways upon stimulation by different doses of sphingosine-1-phosphate in endothelial cells. *Exp Physiol* **100**: 95-107, 2015.

37. Li X, Stankovic M, Bonder CS, Hahn CN, Parsons M, Pitson SM, Xia P, Proia RL, Vadas MA, Gamble JR. Basal and angiopoietin-1-mediated endothelial permeability is regulated by sphingosine kinase-1. *Blood* **111**: 3489-3497, 2008.

38. Litwin M, Clark K, Noack L, Furze J, Berndt M, Albelda S, Vadas M, Gamble J. Novel cytokine-independent induction of endothelial adhesion molecules regulated by platelet/endothelial cell adhesion molecule (CD31). *The Journal of cell biology* **139**: 219-228, 1997.

39. Liu H, Sugiura M, Nava VE, Edsall LC, Kono K, Poulton S, Milstien S, Kohama T, Spiegel S. Molecular cloning and functional characterization of a novel mammalian sphingosine kinase type 2 isoform. *The Journal of biological chemistry* **275**: 19513-19520, 2000.

40. Liu Y, Wada R, Yamashita T, Mi Y, Deng CX, Hobson JP, Rosenfeldt HM, Nava VE, Chae SS, Lee MJ, Liu CH, Hla T, Spiegel S, Proia RL. Edg-1, the G protein-coupled receptor for sphingosine-1-phosphate, is essential for vascular maturation. *The Journal of clinical investigation* **106**: 951-961, 2000.

41. Lum H, Malik AB. Regulation of vascular endothelial barrier function. *The American journal of physiology* **267**: L223-241, 1994.

42. Maceyka M, Alvarez SE, Milstien S, Spiegel S. Filamin A links sphingosine kinase 1 and sphingosine-1-phosphate receptor 1 at lamellipodia to orchestrate cell migration. *Molecular and cellular biology* **28**: 5687-5697, 2008.

43. Maceyka M, Milstien S, Spiegel S. Sphingosine-1-phosphate: the Swiss army knife of sphingolipid signaling. *Journal of lipid research* **50 Suppl**: S272-276, 2009.

44. Maceyka M, Sankala H, Hait NC, Le Stunff H, Liu H, Toman R, Collier C, Zhang M, Satin LS, Merrill AH, Jr., Milstien S, Spiegel S. SphK1 and SphK2, sphingosine kinase isoenzymes with opposing functions in sphingolipid metabolism. *The Journal of biological chemistry* **280**: 37118-37129, 2005.

45. Maines LW, French KJ, Wolpert EB, Antonetti DA, Smith CD. Pharmacologic manipulation of sphingosine kinase in retinal endothelial cells: implications for angiogenic ocular diseases. *Investigative ophthalmology & visual science* **47**: 5022-5031, 2006.

46. McVerry BJ, Peng X, Hassoun PM, Sammani S, Simon BA, Garcia JG. Sphingosine 1-phosphate reduces vascular leak in murine and canine models of acute lung injury. *Am J Respir Crit Care Med* **170**: 987-993, 2004.

47. Mehta D, Malik AB. Signaling mechanisms regulating endothelial permeability. *Physiological reviews* **86**: 279-367, 2006.

48. Melendez AJ, Carlos-Dias E, Gosink M, Allen JM, Takacs L. Human sphingosine kinase: molecular cloning, functional characterization and tissue distribution. *Gene* **251**: 19-26, 2000.

49. Mizugishi K, Yamashita T, Olivera A, Miller GF, Spiegel S, Proia RL. Essential role for sphingosine kinases in neural and vascular development. *Molecular and cellular biology* **25**: 11113-11121, 2005.

50. Murakami M, Nguyen LT, Zhuang ZW, Moodie KL, Carmeliet P, Stan RV, Simons M. The FGF system has a key role in regulating vascular integrity. *The Journal of clinical investigation* **118**: 3355-3366, 2008.

51. Nagy JA, Benjamin L, Zeng H, Dvorak AM, Dvorak HF. Vascular permeability, vascular hyperpermeability and angiogenesis. *Angiogenesis* **11**: 109-119, 2008.

52. Olivera A, Eisner C, Kitamura Y, Dillahunt S, Allende L, Tuymetova G, Watford W, Meylan F, Diesner SC, Li L, Schnermann J, Proia RL, Rivera J. Sphingosine kinase 1 and sphingosine-1-phosphate receptor 2 are vital to recovery from anaphylactic shock in mice. *The Journal of clinical investigation* **120**: 1429-1440, 2010.

53. Olivera A, Mizugishi K, Tikhonova A, Ciaccia L, Odom S, Proia RL, Rivera J. The sphingosine kinase-sphingosine-1-phosphate axis is a determinant of mast cell function and anaphylaxis. *Immunity* **26**: 287-297, 2007.

54. Parham KA, Zebol JR, Tooley KL, Sun WY, Moldenhauer LM, Cockshell MP, Gliddon BL, Moretti PA, Tigyi G, Pitson SM, Bonder CS. Sphingosine 1-phosphate is a ligand for peroxisome proliferator-activated receptor-gamma that regulates neoangiogenesis. *FASEB journal : official publication of the Federation of American Societies for Experimental Biology*, 2015.

55. Pitman MR, Pitson SM. Inhibitors of the sphingosine kinase pathway as potential therapeutics. *Current cancer drug targets* **10**: 354-367, 2010.

56. Pitman MR, Powell JA, Coolen C, Moretti PA, Zebol JR, Pham DH, Finnie JW, Don AS, Ebert LM, Bonder CS, Gliddon BL, Pitson SM. A selective ATP-competitive sphingosine kinase inhibitor demonstrates anti-cancer properties. *Oncotarget* **6**: 7065-7083, 2015.

57. Pitson SM, Moretti PA, Zebol JR, Lynn HE, Xia P, Vadas MA, Wattenberg BW. Activation of sphingosine kinase 1 by ERK1/2-mediated phosphorylation. *The EMBO journal* **22**: 5491-5500, 2003.

58. Pitson SM, Pebay A. Regulation of stem cell pluripotency and neural differentiation by lysophospholipids. *Neuro-Signals* **17**: 242-254, 2009.

59. Pizurki L, Zhou Z, Glynos K, Roussos C, Papapetropoulos A. Angiopoietin-1 inhibits endothelial permeability, neutrophil adherence and IL-8 production. *British journal of pharmacology* **139**: 329-336, 2003.

60. Pyne NJ, Pyne S. Sphingosine 1-phosphate and cancer. *Nature reviews Cancer* **10**: 489-503, 2010.

61. Rasband WS. ImageJ, U. S. National Institutes of Health, Bethesda, Maryland, USA, http://rsb.info.nih.gov/ij/, 1997-2012.

62. Rotrosen D, Gallin JI. Histamine type I receptor occupancy increases endothelial cytosolic calcium, reduces F-actin, and promotes albumin diffusion across cultured endothelial monolayers. *The Journal of cell biology* **103**: 2379-2387, 1986.

63. Sammani S, Moreno-Vinasco L, Mirzapoiazova T, Singleton PA, Chiang ET, Evenoski CL, Wang T, Mathew B, Husain A, Moitra J, Sun X, Nunez L, Jacobson JR, Dudek SM, Natarajan V, Garcia JG. Differential effects of sphingosine 1-phosphate receptors on airway and vascular barrier function in the murine lung. *American journal of respiratory cell and molecular biology* **43**: 394-402, 2010.

64. Sanchez T, Hla T. Structural and functional characteristics of S1P receptors. *J Cell Biochem* **92**: 913-922, 2004.

65. Schnute ME, McReynolds MD, Kasten T, Yates M, Jerome G, Rains JW, Hall T, Chrencik J, Kraus M, Cronin CN, Saabye M, Highkin MK, Broadus R, Ogawa S, Cukyne K, Zawadzke LE, Peterkin V, Iyanar K, Scholten JA, Wendling J, Fujiwara H, Nemirovskiy O, Wittwer AJ, Nagiec MM. Modulation of cellular S1P levels with a novel, potent and specific inhibitor of sphingosine kinase-1. *The Biochemical journal* **444**: 79-88, 2012.

66. Schweitzer KM, Vicart P, Delouis C, Paulin D, Drager AM, Langenhuijsen MM, Weksler BB. Characterization of a newly established human bone marrow endothelial cell line: distinct adhesive properties for hematopoietic progenitors compared with human umbilical vein endothelial cells. *Laboratory investigation; a journal of technical methods and pathology* **76**: 25-36, 1997.

67. Sensken SC, Bode C, Nagarajan M, Peest U, Pabst O, Graler MH. Redistribution of sphingosine 1-phosphate by sphingosine kinase 2 contributes to lymphopenia. *Journal of immunology* **184**: 4133-4142, 2010.

68. Siow D, Wattenberg B. The compartmentalization and translocation of the sphingosine kinases: mechanisms and functions in cell signaling and sphingolipid metabolism. *Critical reviews in biochemistry and molecular biology* **46**: 365-375, 2011.

69. Stolwijk JA, Matrougui K, Renken CW, Trebak M. Impedance analysis of GPCR-mediated changes in endothelial barrier function: overview and fundamental considerations for stable and reproducible measurements. *Pflugers Arch* **467**: 2193-2218, 2015.

70. Strader CR, Pearce CJ, Oberlies NH. Fingolimod (FTY720): a recently approved multiple sclerosis drug based on a fungal secondary metabolite. *J Nat Prod* **74**: 900-907, 2011.

71. Strub GM, Paillard M, Liang J, Gomez L, Allegood JC, Hait NC, Maceyka M, Price MM, Chen Q, Simpson DC, Kordula T, Milstien S, Lesnefsky EJ, Spiegel S. Sphingosine-1-phosphate produced by sphingosine kinase 2 in mitochondria interacts with prohibitin 2 to regulate complex IV assembly and

respiration. *FASEB journal : official publication of the Federation of American Societies for Experimental Biology* **25**: 600-612, 2011.

72. Sun M, Fu H, Cheng H, Cao Q, Zhao Y, Mou X, Zhang X, Liu X, Ke Y. A dynamic real-time method for monitoring epithelial barrier function in vitro. *Analytical biochemistry* **425**: 96-103, 2012.

73. Sun WY, Abeynaike LD, Escarbe S, Smith CD, Pitson SM, Hickey MJ, Bonder CS. Rapid histamine-induced neutrophil recruitment is sphingosine kinase-1 dependent. *The American journal of pathology* **180**: 1740-1750, 2012.

74. Taha TA, Hannun YA, Obeid LM. Sphingosine kinase: biochemical and cellular regulation and role in disease. *Journal of biochemistry and molecular biology* **39**: 113-131, 2006.

75. Tauseef M, Kini V, Knezevic N, Brannan M, Ramchandaran R, Fyrst H, Saba J, Vogel SM, Malik AB, Mehta D. Activation of sphingosine kinase-1 reverses the increase in lung vascular permeability through sphingosine-1-phosphate receptor signaling in endothelial cells. *Circulation research* **103**: 1164-1172, 2008.

76. Tiruppathi C, Malik AB, Del Vecchio PJ, Keese CR, Giaever I. Electrical method for detection of endothelial cell shape change in real time: assessment of endothelial barrier function. *Proceedings of the National Academy of Sciences of the United States of America* **89**: 7919-7923, 1992.

77. Tozer GM, Kanthou C, Baguley BC. Disrupting tumour blood vessels. *Nature reviews Cancer* **5**: 423-435, 2005.

78. Venant H, Rahmaniyan M, Jones EE, Lu P, Lilly MB, Garrett-Mayer E, Drake RR, Kraveka JM, Smith CD, Voelkel-Johnson C. The Sphingosine Kinase 2 Inhibitor ABC294640 Reduces the Growth of Prostate Cancer Cells and Results in Accumulation of Dihydroceramides In Vitro and In Vivo. *Mol Cancer Ther*, 2015.

79. Venkataraman K, Lee YM, Michaud J, Thangada S, Ai Y, Bonkovsky HL, Parikh NS, Habrukowich C, Hla T. Vascular endothelium as a contributor of plasma sphingosine 1-phosphate. *Circulation research* **102**: 669-676, 2008.

80. Xiong Y, Yang P, Proia RL, Hla T. Erythrocyte-derived sphingosine 1-phosphate is essential for vascular development. *The Journal of clinical investigation* **124**: 4823-4828, 2014.

81. Yang L, Yatomi Y, Miura Y, Satoh K, Ozaki Y. Metabolism and functional effects of sphingolipids in blood cells. *British journal of haematology* **107**: 282-293, 1999.

82. Yatomi Y, Igarashi Y, Yang L, Hisano N, Qi R, Asazuma N, Satoh K, Ozaki Y, Kume S. Sphingosine 1-phosphate, a bioactive sphingolipid abundantly stored in platelets, is a normal constituent of human plasma and serum. *Journal of biochemistry* **121**: 969-973, 1997.

83. Zipfel WR, Williams RM, Webb WW. Nonlinear magic: multiphoton microscopy in the biosciences. *Nature biotechnology* **21**: 1369-1377, 2003.

FIGURE LEGENDS

Figure 1. Histamine rapidly decreases HUVEC barrier integrity via histamine receptor 1. **(A)** HUVEC were seeded into the E-Plate 16 wells at various concentrations (0.5, 1.0, 2.5 and 5 x 10^4 cells/well) and cell index readings were monitored for 20 hours. **(B)** HUVEC were treated with 12.5 μM histamine or equivalent vehicle control. Cell index readings were monitored for 25 minutes following treatment. **(C)** HUVEC were treated with or without 10 μM of the histamine receptor 1 (H1R) inhibitor chlorpheniramine prior to the addition of 12.5 μM histamine. **(D)** HUVEC were treated with or without 10 μM of the histamine receptor 2 inhibitor (H2R) cimetidine prior to the addition of 12.5 μM histamine. **(E)** Changes in barrier integrity were quantified using an area under the curve analysis (cell index x minutes). Each treatment was performed in duplicate on three biologically different HUVEC donors. Error bars represent standard error of the mean. * $p < 0.05$

Figure 2. The SK-1 inhibitor PF543 causes a significant decrease in HUVEC barrier integrity. HUVEC were treated with PF543 at **(A)** 10 nM, **(B)** 25 nM, **(C)** 50 nM and **(D)** 100 nM and the equivalent concentration of the vehicle. **(E)** Changes in barrier integrity were quantified using an area under the curve analysis (cell index x minutes). Each treatment was performed in duplicate on three HUVEC donors. Error bars represent standard error of the mean. * $p < 0.05$

Figure 3. The SK-2 inhibitor ABC294640 causes a significant decrease in HUVEC barrier integrity. HUVEC were treated with ABC294640 at **(A)** 5 μM, **(B)** 10 μM, **(C)** 20 μM and **(D)** 40 μM and the equivalent concentration of the vehicle. **(E)** Changes in barrier integrity were quantified using an area under the curve analysis (cell index x minutes). Each treatment was performed in duplicate on three HUVEC donors. Error bars represent standard error of the mean. * $p < 0.05$

Figure 4. Combination of PF543 and ABC294640 enhances the decrease in HUVEC barrier integrity. HUVEC were treated with **(A)** PF543 at 100 nM, **(B)** ABC294640 at 20 μM or **(C)** a combination of both these inhibitors at the same concentrations**.** The equivalent concentration of each vehicle was also included. **(E)** Changes in barrier integrity were quantified using an area under the curve analysis (cell index x minutes). Each treatment was performed in duplicate on three HUVEC donors. Error bars represent standard error of the mean. * $p < 0.05$

Figure 5. The SK-1/2 inhibitor SKi has no effect on HUVEC barrier integrity. HUVEC treated with SKi at **(A)** 5 μM, **(B)** 10 μM, **(C)** 20 μM and **(D)** 40 μM and the equivalent concentration of the vehicle. **(E)** Changes in barrier integrity were quantified using an area under the curve analysis (cell index x minutes). Each treatment was performed in duplicate on three HUVEC donors. Error bars represent standard error of the mean.

Figure 6. The SK-1/2 inhibitor MP-A08 causes a significant decrease in HUVEC barrier integrity. HUVEC were treated with MP-A08 at **(A)** 5 μM, **(B)** 10 μM, **(C)** 20 μM and **(D)** 40 μM and the equivalent concentration of the vehicle. **(E)** Changes in barrier integrity were quantified using an area under the curve analysis (cell index x minutes). Each treatment was

performed in duplicate on three HUVEC donors. Error bars represent standard error of the mean. * $p < 0.05$

Figure 7. The SK inhibitors have varying effects on BMEC barrier integrity. BMEC were treated with **(A)** PF543 at 100 nM, **(B)** ABC294640 at 20 μM, **(C)** SKi at 40 μM and **(D)** MP-A08 at 40 μM and the equivalent concentration of each vehicle. **(E)** Changes in barrier integrity were quantified using an area under the curve analysis (cell index x minutes). Each treatment was performed in duplicate on three independent experiments. Error bars represent standard error of the mean. * $p < 0.05$

Figure 8. *Sphk1*$^{-/-}$ and *Sphk2*$^{-/-}$ mice do not exhibit increased microvascular leakage of 150 kDa FITC-Dextran. WT, *Sphk1*$^{-/-}$ and *Sphk2*$^{-/-}$ mice were injected with 150 kDa FITC-Dextran and fluorescent images of the ear vasculature were taken over time. Representative images from a **(A)** WT, **(B)** *Sphk1*$^{-/-}$ and **(C)** *Sphk2*$^{-/-}$ mouse are shown, with only the 0 minute, 5 minute and 15 minutes time points represented (scale bars indicate 100 μm). **(D)** Data are shown as the mean normalised fluorescence area ± standard error of the mean (n = 4).

Figure 9. *Sphk1*$^{-/-}$ but not *Sphk2*$^{-/-}$ mice exhibit increased microvascular leakage of 70 kDa FITC-Dextran. WT, *Sphk1*$^{-/-}$ and *Sphk2*$^{-/-}$ mice were injected with 70 kDa FITC-Dextran and fluorescent images of the ear vasculature were taken over time. Representative images from a **(A)** WT, **(B)** *Sphk1*$^{-/-}$ and **(C)** *Sphk2*$^{-/-}$ mouse are shown, with only the 0 minute, 5 minute and 15 minutes time points represented (scale bars indicate 100 μm). **(D)** Data are shown as the mean normalised fluorescence area ± standard error of the mean (n = 4-6). ** $p < 0.001$. **(E)** Data are shown at the 10 min time point for normalised fluorescence area for each male and female mouse in the WT and *Sphk1*$^{-/-}$ group.

Figure 10. *Sphk1*$^{-/-}$ but not *Sphk2*$^{-/-}$ mice exhibit increased microvascular leakage of 40 kDa FITC-Dextran. WT, *Sphk1*$^{-/-}$ and *Sphk2*$^{-/-}$ mice were injected with 40 kDa FITC-Dextran and fluorescent images of the ear vasculature were taken over time. Representative images from a **(A)** WT, **(B)** *Sphk1*$^{-/-}$ and **(C)** *Sphk2*$^{-/-}$ mouse are shown, with only the 0 minute, 5 minute and 15 minutes time points represented (scale bars indicate 100 μm). **(D)** Data are shown as the mean normalised fluorescence area ± standard error of the mean (n = 5). *$p < 0.05$

Supplementary Figure 1. HUVEC treated with SK-1 inhibitor PF543 exhibit no sign of long-term cell toxicity. HUVEC were treated with PF543 at **(A)** 10 nM, **(B)** 25 nM, **(C)** 50 nM, **(D)** 100 nM and the equivalent concentration of the vehicle. Cell index readings were monitored for 12 hours following treatment, (n = 3)

Supplementary Figure 2. HUVEC treated with SK-2 inhibitor ABC294640 exhibit no sign of long-term cell toxicity. HUVEC were treated with ABC294640 at **(A)** 5 μM, **(B)** 10 μM, **(C)** 20 μM, **(D)** 40 μM and the equivalent concentration of the vehicle. Cell index readings were monitored for 12 hours following treatment, (n = 3).

Supplementary Figure 3. HUVEC treated with a combination of PF543 and ABC294640 exhibit no sign of long-term cell toxicity. HUVEC were treated with **(A)** PF543 at 100 nM, **(B)** ABC294640 at 20 μM, **(C)** a combination of both inhibitors at the same concentration and the equivalent concentration of each vehicle. Cell index readings were monitored for 12 hours following treatment, (n = 3).

Supplementary Figure 4. HUVEC treated with SK-1/2 inhibitor SKi exhibit no sign of long-term cell toxicity. HUVEC were treated with SKi at **(A)** 5 μM, **(B)** 10 μM, **(C)** 20 μM, **(D)** 40

μM and the equivalent concentration of the vehicle. Cell index readings were monitored for 12 hours following treatment, (n = 3).

Supplementary Figure 5. HUVEC treated with SK-1/2 inhibitor MP-A08 exhibit no sign of long-term cell toxicity. HUVEC were treated with MP-A08 at **(A)** 5 μM, **(B)** 10 μM, **(C)** 20 μM, **(D)** 40 μM and the equivalent concentration of the vehicle. Cell index readings were monitored for 12 hours following treatment, (n = 3).

Supplementary Figure 6. BMEC only exhibit signs of long-term cell toxicity to the inhibitor SKi. BMEC were treated with **(A)** PF543 at 100 nM, **(B)** ABC294640 at 20 μM, **(C)** SKi at 40 μM, **(D)** MP-A08 at 40 μM and the equivalent concentration of the vehicle. Cell index readings were monitored for 12 hours following treatment, (n = 3).

Supplementary Figure 7. Blood vessel composition was similar in mice assessed for intravital microscopy assay. The proportion of small, medium or large vessels per mouse was calculated for each size of FITC-Dextran and for each genotype. Error bars represent standard error of the mean. n = 4 (150 kDa and 70 kDa) and n = 5 (40 kDa), $*p < 0.05$.

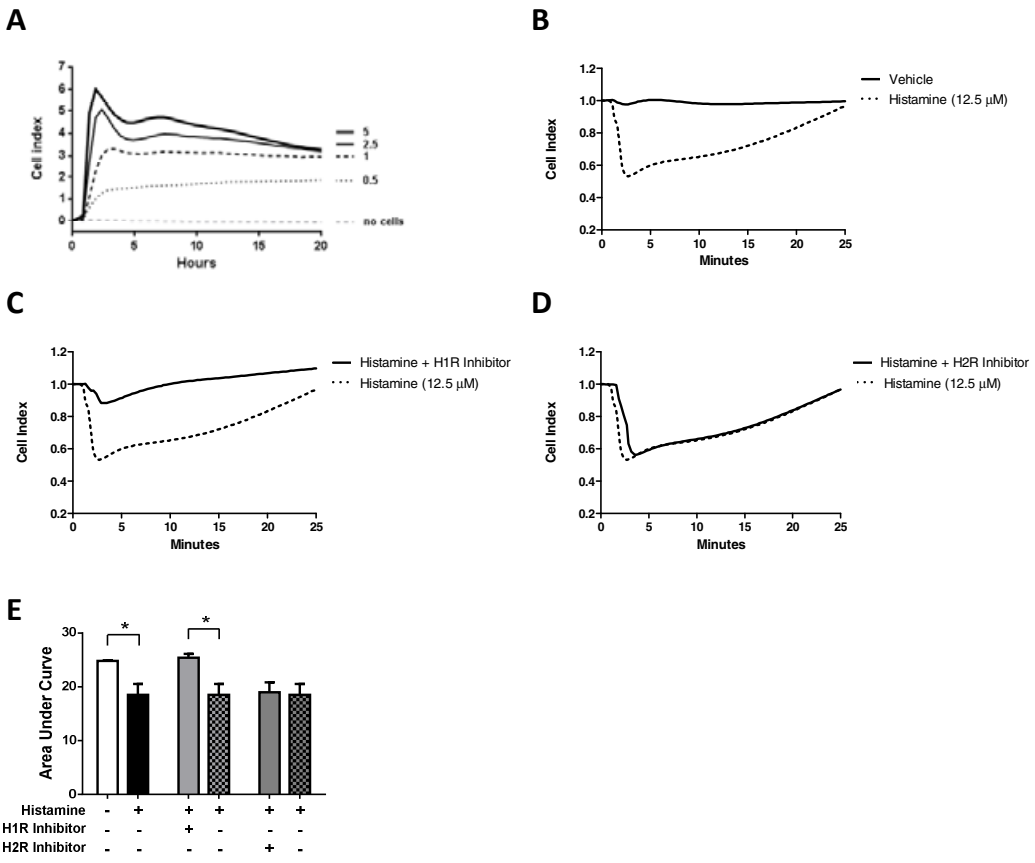

Figure 1

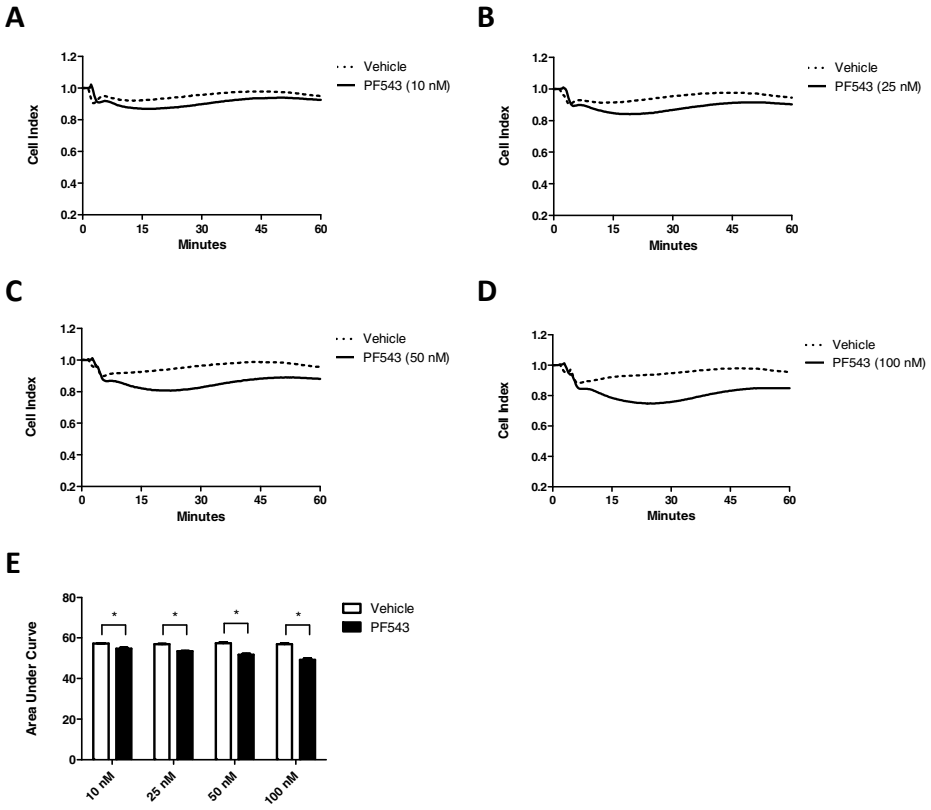

Figure 2

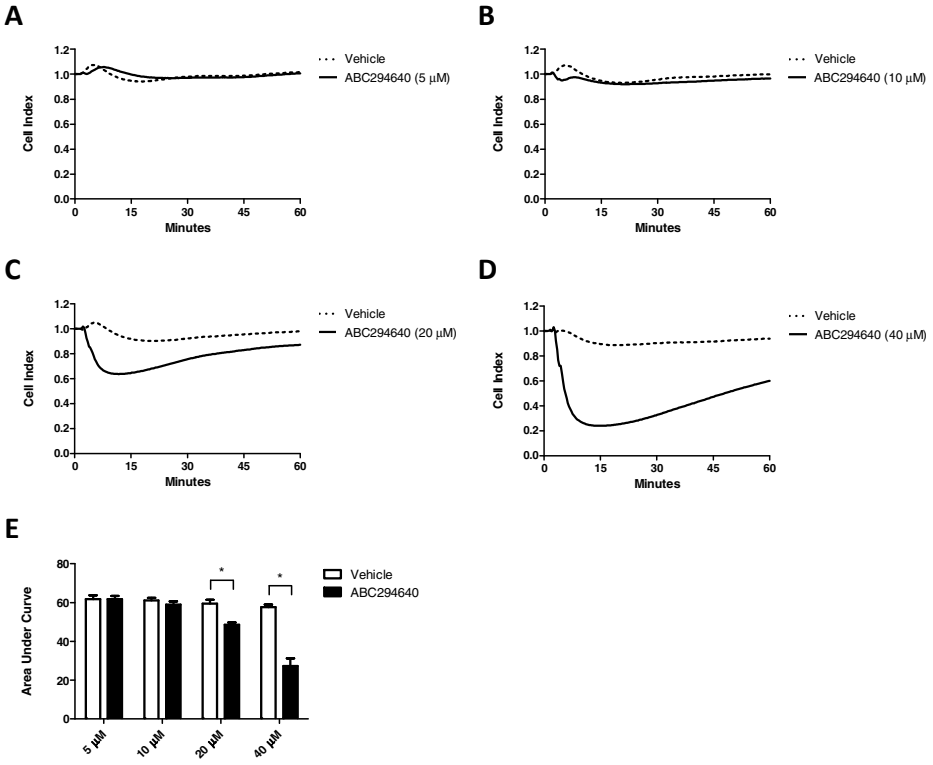

Figure 3

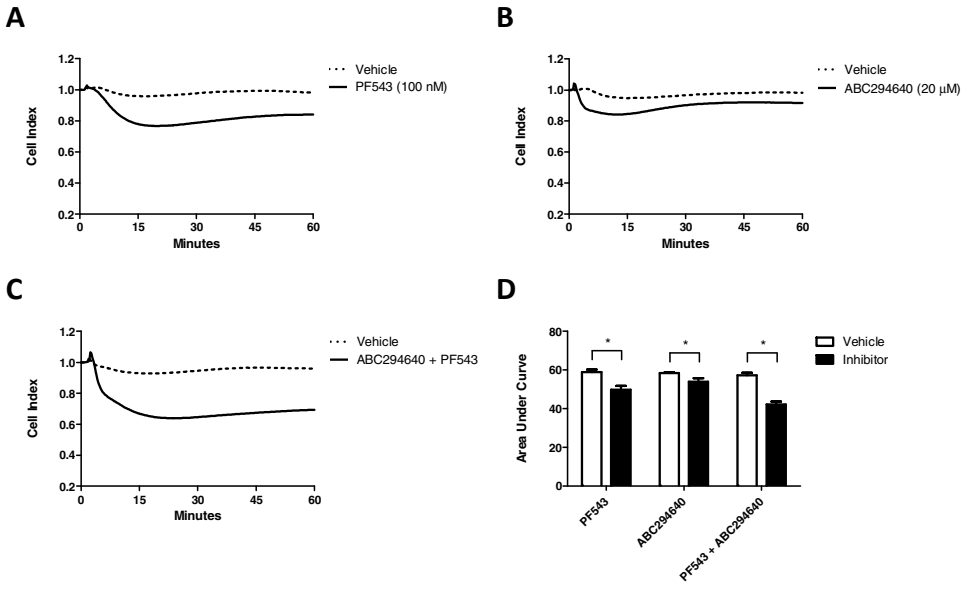

Figure 4

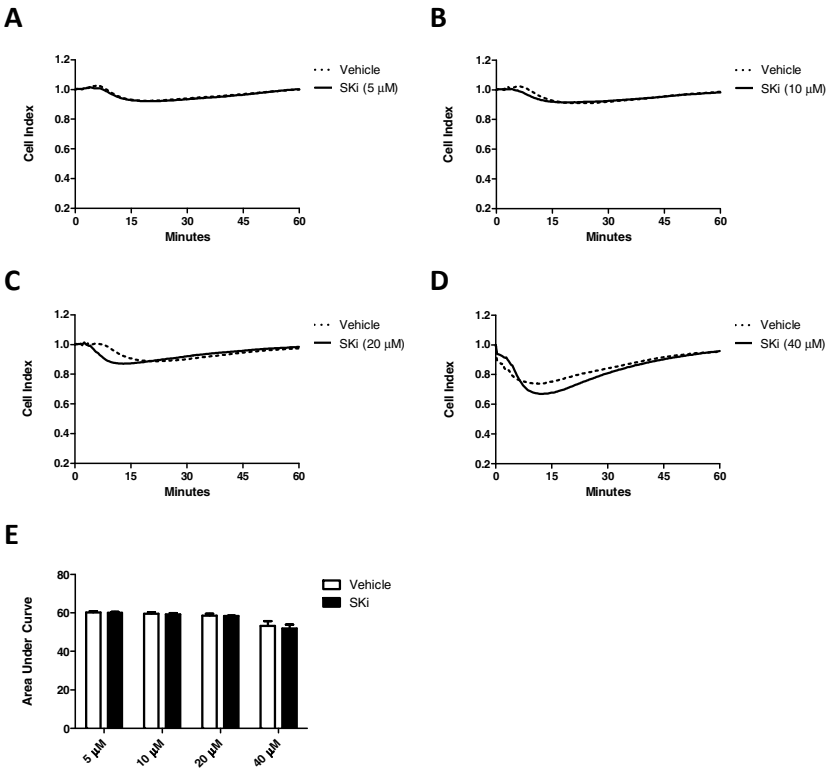

Figure 5

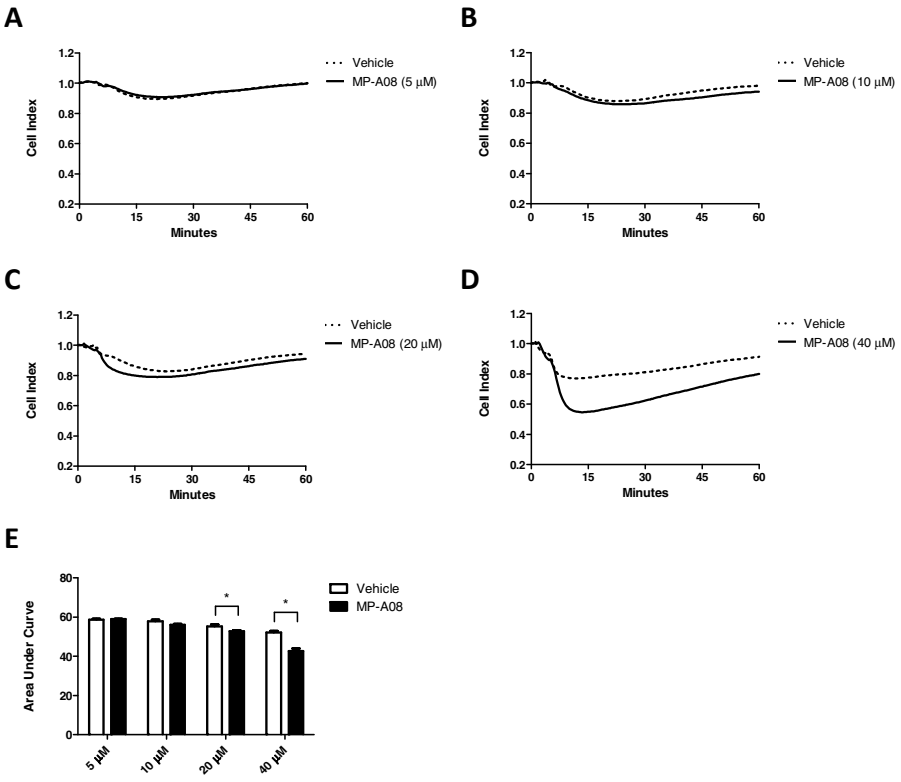

Figure 6

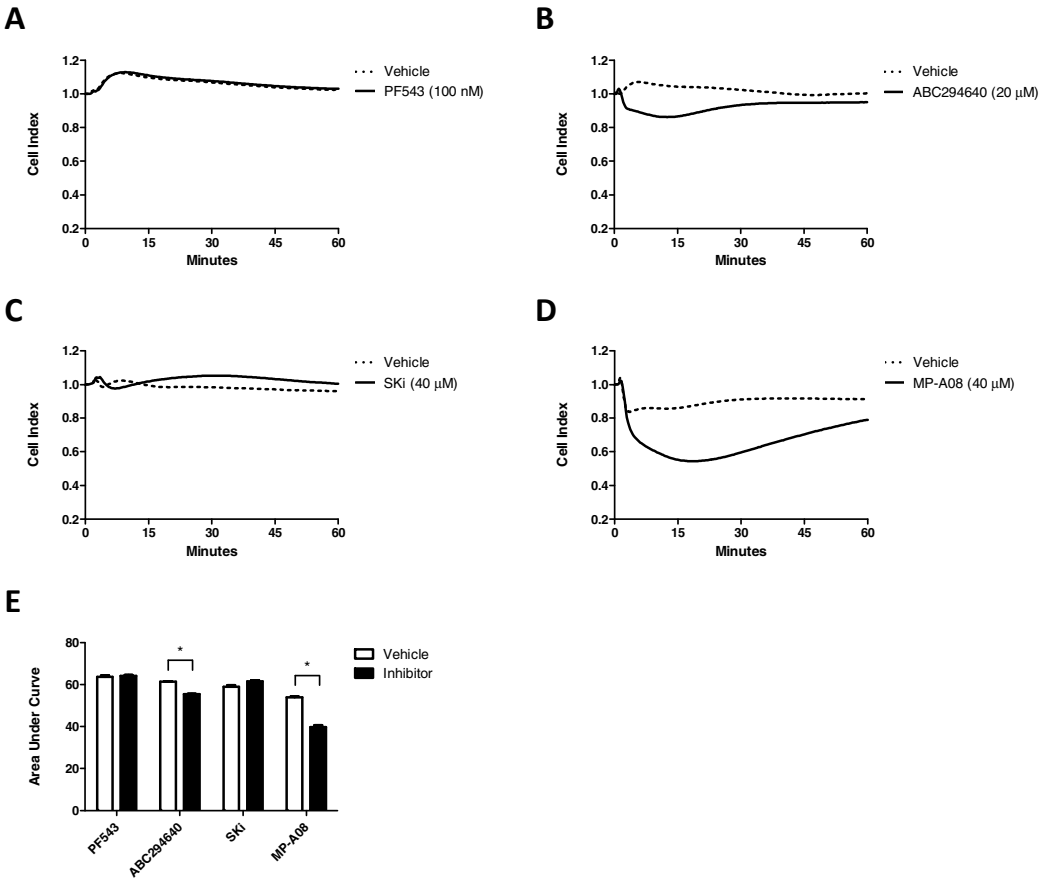

Figure 7

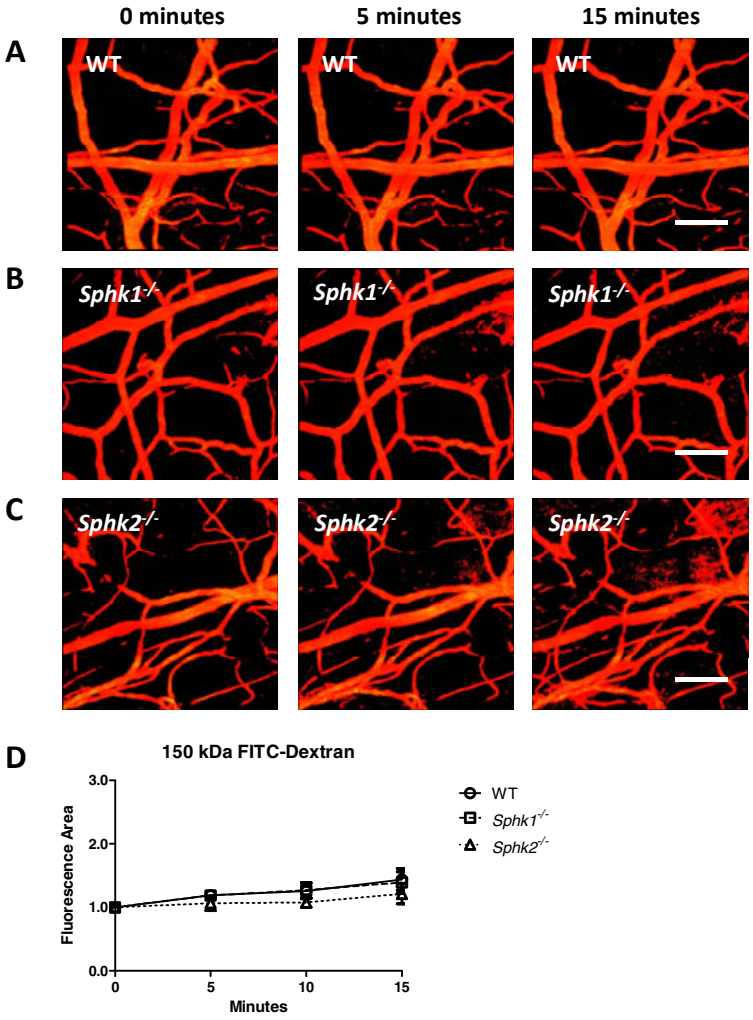

Figure 8

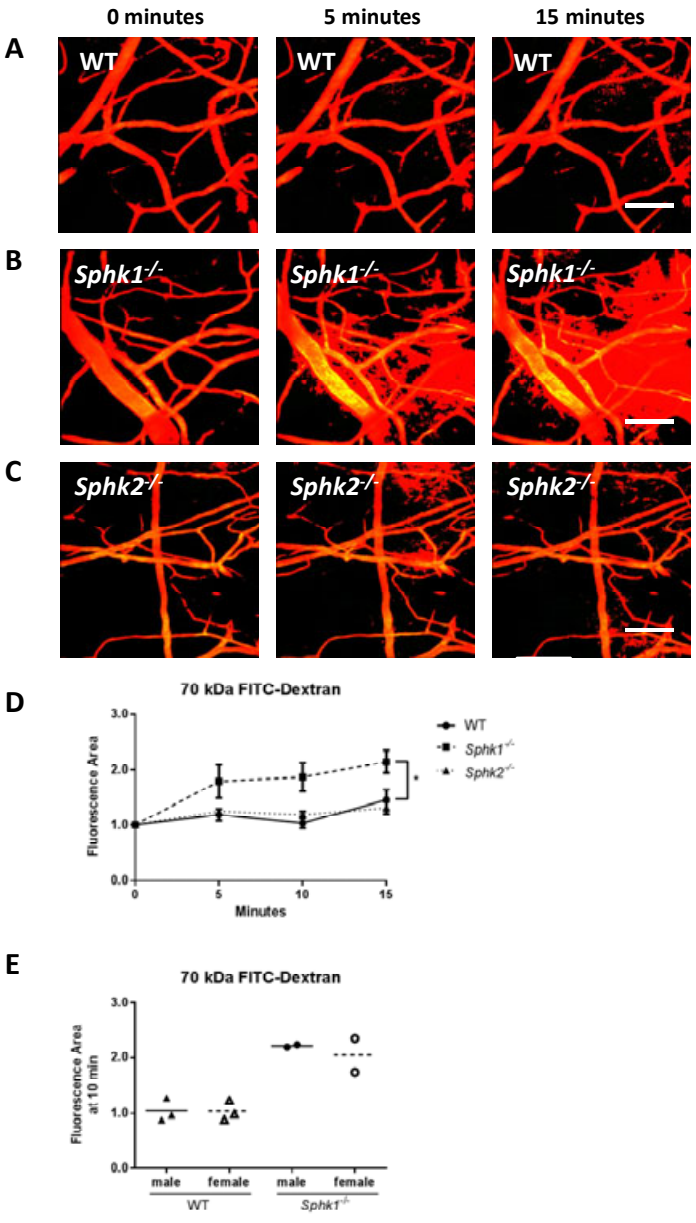

Figure 9

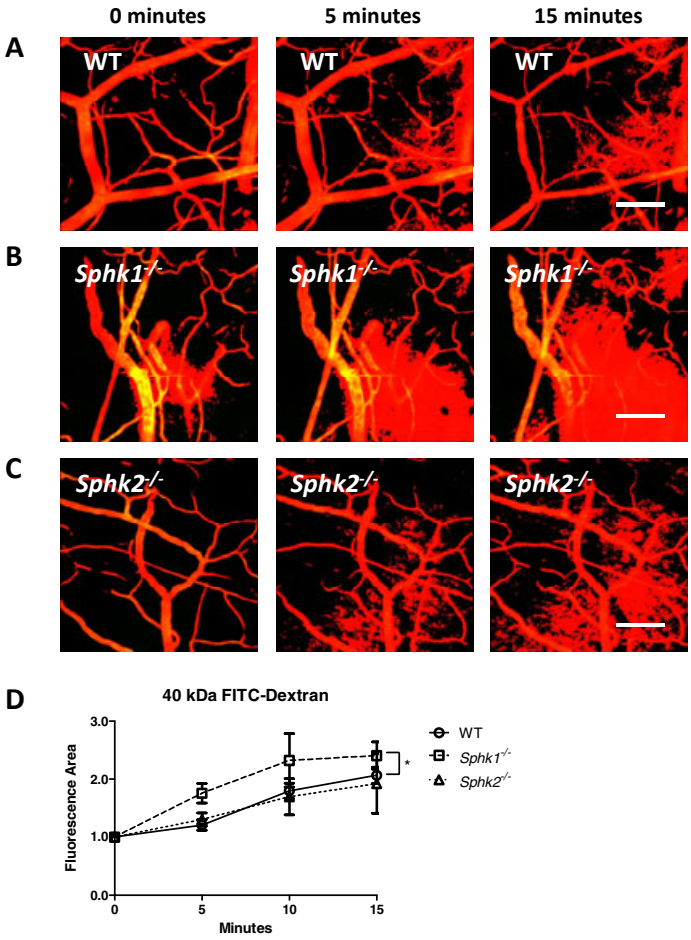

Figure 10